Available online at www.sciencedirect.com
SCIENCE DIRECT®
Journal of Luminescence 118 (2006) 173–178
JOURNAL OF LUMINESCENCE
www.elsevier.com/locate/jlumin

Green emitting long lasting phosphorescence (LLP) properties of $Mg_2SnO_4:Mn^{2+}$ phosphor

Bingfu Lei[a,b], Bin Li[a,*], Xiaojun Wang[a], Wenlian Li[a]

[a]*Key Laboratory of Excited State Processes, Changchun Institute of Optics Fine Mechanics and Physics, Chinese Academy of Sciences, Changchun, Jilin 130033, PR China*

[b]*Graduate School of the Chinese Academy of Sciences, Chinese Academy of Sciences, Beijing 100039, PR China*

Received 29 March 2005
Available online 4 January 2006

Abstract

A novel long-lasting phosphorescence phosphor, Mn^{2+}-activated Mg_2SnO_4, has been synthesized and its optical properties have been investigated. The $Mg_2SnO_4:Mn^{2+}$ emits green light with high luminance, upon UV irradiation, centered at 499 nm from the spin forbidden transitions of the d-electrons in Mn^{2+} ions. The CIE chromaticity coordinates of the $Mg_2SnO_4:Mn^{2+}$ phosphor are $x = 0.0875$ and $y = 0.6083$ under 254 nm UV excitation. The phosphorescence can be observed by the naked eyes (0.32 mcd/m^2) in the dark clearly for over 5 h after the 5 min UV irradiation. Thermoluminescence has been studied and the mechanism of the long-lasting phosphorescence has been discussed.

Keywords: $Mg_2SnO_4:Mn^{2+}$; Afterglow; Thermoluminescence; Long-lasting phosphor

1. Introduction

Long-lasting phosphorescence (LLP) phosphors are a class of luminescent materials, which attract the interest of researchers due to their various applications, such as emergent lighting, display, detection of high-energy rays (e.g. UV, X-ray, and β-ray), multidimensional optical memory, and imaging storage [1,2]. Theoretically, LLP originate from the thermal stimulated recombination of holes and electrons stored in the traps, the long-lived excited state at room temperature [3]. It is expected that the LLP can be observed from the phosphors if there exist adequate hole traps and electron traps with suitable depth. Based on this principle, researchers in this field have developed various kinds of LLP phosphors with different lattice host and different activators. Several hundred papers have been published in search

*Corresponding author. Tel.: +86 431 6176935; fax: +86 431 6176935.
E-mail addresses: ray-lei@vip.sina.com (B. Lei), lib020@ciomp.ac.cn (B. Li).

0022-2313/$ - see front matter © 2005 Published by Elsevier B.V.
doi:10.1016/j.jlumin.2005.08.010

for better LLP phosphors and for better understanding their mechanisms, however, progress in developing the LLP materials with excellent optical properties (e.g., high luminance and long persistent time) has still been slow because the nature of traping and their mechanisms of capturing energy are complicated and not totally understood [4]. To the present time, the most efficient LLP phosphors are still based on alkaline-earth aluminates, for example, $SrAl_2O_4$:Dy,Eu (green) [5], $CaAl_2O_4$:Nd,Eu (violet) [6], and $Sr_4Al_{14}O_{25}$:Dy,Eu (blue) [7]. The brightness of this kind of phosphor is 10 times better than the previous sulfide phosphors and the persistent time is well over 10 h after UV excitation and without doping any radioactive materials [5,8].

Generally, the luminescent properties of phosphors are strongly dependent on the crystal structure of the host materials. Finding a right matrix is still a critical step to obtain rare-earth ions or transition metal ions-doped LLP with excellent properties. $(SnO_4)^{4-}$ anions are reported to be optically inert and could be a candidate for host materials [9–11]. Recently, luminescence properties of manganese-doped magnesium tin oxide, under vacuum ultraviolet ray and low-voltage electron excitation, have been reported. It was found that the Mg_2SnO_4:Mn phosphor presented higher emission intensity and a shorter decay time than that of the commercial Zn_2SiO_4:Mn phosphor [10]. Mg_2SnO_4 is a chemically stable host with a cubic inverse spinel crystal structure that belongs to the space group Fd3m [10,12,13]. The unit cell has 96 cation sites with 24 being occupied by the cations; 8 of 64 tetrahedral sites by Mg^{2+}, and 16 of 32 octahedral sites by other Mg^{2+} and Sn^{4+}. In addition to the large number of unoccupied sites, the degree of cation disorder can be considerable (as large as 30%), so that a large number of defects can be created [14–17]. Some of these defects serve as electron or hole traps. For example, an Mg^{2+} at an Sn^{4+} site can trap a hole; while a Sn^{4+} at an Mg^{2+} site will form an electron trap. Oxygen vacancies may also serve as F-center-like electron traps [17,18]. Therefore this oxide matrix is expected to be a good candidate for LLP phosphor. To our best knowledge, there is no literature reported yet about the LLP properties of SnO_4^{4-} anions-based oxides. In this paper, the optical property of Mn^{2+}-doped Mg_2SnO_4 LLP is reported upon ultra-violet excitation. The mechanisms of traping and detraping processes are also discussed through thermoluminescence (TL) study.

2. Experimental

2.1. Sample preparation

The powder samples were prepared using the conventional solid-state reaction method. The starting materials used in the preparation of these phosphors were MgO (A.R.), SnO_2 (A.R.), and $Mn(CH_3COO)_2 \cdot 4H_2O$ (A.R.). The Mn^{2+} dopant concentrations range from 0.01 to 10 mol% of Mg^{2+} ions in Mg_2SnO_4. Preweighed powders were mixed thoroughly in ethanol in an agate mortar and dried to drive off the solvent and successively heat-treated at several conditions of temperature and duration time using alumina crucibles with alumina lids in an air atmosphere, followed by an additional grinding and firing in reduction atmosphere. At this step, the weak-reducing atmosphere is created by mixing high-purity kryptol in high temperatures.

2.2. Measurements

The X-ray powder diffraction patterns were obtained by a Rigaku Model D/max-II B X-ray diffractometer running at 40 kV and 20 mA. The scanning speed was 4°/min with a step of 0.02°(2θ). The X-ray radiation wavelength is 0.15405 nm from Cu $K\alpha_1$.

For photoluminescence (PL) measurements, the emission and excitation spectra were recorded at room temperature using a Hitachi F-4500 fluorescence spectrophotometer (resolution: 0.2 nm) with a 150 W Xe lamp as the excitation source. The CIE value was obtained using the Hitachi MPF-fluorescence spectrophotometer.

The afterglow emission spectra and afterglow intensity decay curves were measured on the same Hitachi F-4500 fluorescence spectrophotometer using our previously reported method [19]. The

UV excitation light of the sample was switched off after 5 min irradiation to the sample. The afterglow emissions were recorded by the same spectrofluorometer using the kinetic analysis mode. The integrated area under the afterglow emission bands was plotted as a function of the decay time to serve the afterglow intensity decay curves. The slits were set to be 2.5 and 5 nm for measuring excitation and emission, respectively, during the whole experiment.

TL glow curves were measured using a Thermal Luminescence Meter System (a product of Beijing Nuclear Instrument Factory) equipped with a temperature-controlled oven and a PC data acquisition system (FJ427-A1). The samples were irradiated for 5 min at 254 nm from a 15 W mercury lamp before measurement. All TL spectra were collected at least three times to ensure the accuracy of the features at a linear temperature scanning rate of 2 K/s.

3. Results and discussions

3.1. Crystal structure of phosphor

The orthostannate Mg_2SnO_4 has recently been studied as potential electronic ceramics [20], and a number of techniques for materials synthesis were employed in the Mg_2SnO_4 and other alkaline-earth stannate systems. Interestingly, the structural behavior of orthostannate (Mg_2SnO_4) is totally different from the corresponding Ca, Sr and Ba counterparts. In some case, even the orthostannate cannot be synthesized as a single phase [21,22]. To make sure whether our results are reliable, we have carefully prepared our samples and checked their structure. The X-ray diffraction patterns of 0.25% Mn^{2+}-doped Mg_2SnO_4 sample (the concentration quenching occurs when Mn^{2+} is doped above 0.25%) under different synthesis conditions are shown in Fig. 1. It is clearly shown that the sample synthesized under weak reducing atmosphere (created by high-purity kryptol at high temperature) are chemically and structurally single-phased Mg_2SnO_4 that corresponds to the JCPDS 24-1424 card, while other samples obtained under ambient air or pure H_2 gas have an additional phase, SnO_2 (JCPDS 41-1445) or MgO (JCPDS 45-0946), respectively. The pure Mg_2SnO_4:Mn phosphor yields light bluish white body color, indicating the absent of Mn^{3+} or Mn^{4+}. The samples appear light pink and light gray body colors if sintered under ambient air and H_2 gas, respectively, due to the tin component was reduced. The results are in excellent agreement with those reported by Kim [10].

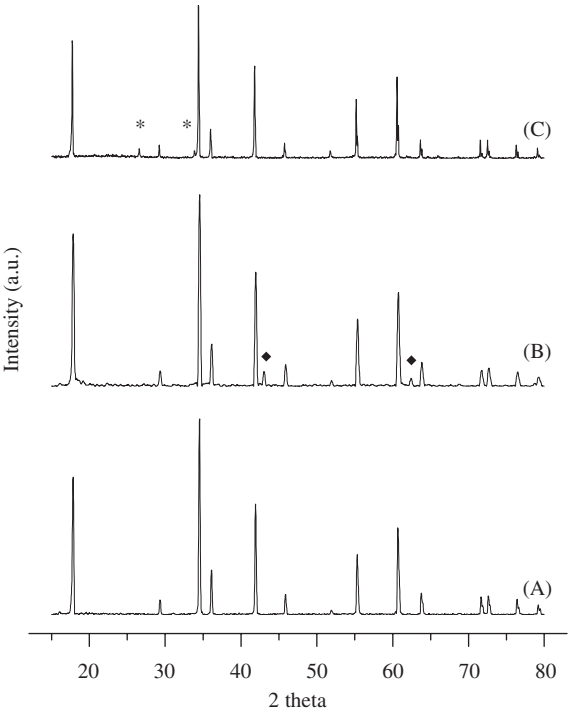

Fig. 1. XRD patterns of 0.25% Mn^{2+}-doped Mg_2SnO_4 phosphor sintered under different condition: (A) weak reducing atmosphere using kryptol; (B) pure H_2 gas; (C) ambient air (◆: MgO, ∗: SnO_2).

3.2. PL properties of Mg_2SnO_4:Mn^{2+} phosphor

A series of Mg_2SnO_4:Mn^{2+} phosphors has been synthesized with the dopant level ranging from 0.01% to 10%. The concentration quenching occurs when Mn^{2+} is doped above 0.25%. The low quenching concentration in this system can be explained by the exchange interaction between the Mn^{2+} ions in tetrahedral sites and the Mn^{2+} ions in octahedral sites [10]. The emission spectrum of

0.25% Mn^{2+}-doped Mg_2SnO_4 phosphor under 267 nm excitation is shown in Fig. 2. The emission spectrum is dominated by a broad band centered at 499 nm plus some weak blue emission. The 499 nm green emission can be attributed to the $^4T_{1g}(G) \rightarrow {}^6A_{1g}(S)$ transition of Mn^{2+} ions occupying the tetrahedral Mg^{2+} sites in the lattice because the luminescence character is consistent with Mn^{2+} emission [10,23]. The weak blue emission of Mg_2SnO_4 phosphor in the emission spectrum is similar to the emission from self-actived $ZnGa_2O_4$ phosphor [24]. The Commission International de 1' Eclairage, France (CIE) chromaticity coordinates are measured at room temperature for the photoluminescence from Mg_2SnO_4:0.25% Mn^{2+} sample with values of $x = 0.0875$ and $y = 0.6083$.

The room temperature excitation spectrum for the Mn^{2+} emission monitored at 499 nm is depicted in Fig. 3. The excitation spectrum was found to be composed of two major peaks at 230 and 267 nm, respectively, plus several weak features located between 360 and 460 nm. The band at 380 nm corresponds to the transition of $^4T_{2g}(^4D) \rightarrow {}^4A_{1g}(^4G)$. The band at 425 nm can be ascribed to the $^4E_{2g}(^4G) \rightarrow {}^4A_{1g}(^4G)$ transition and the band at 445 nm to the $^4T_{2g}(^4G) \rightarrow {}^4T_{1g}(^4G)$ transition [25].

In order to explain the weak blue emission, the undoped Mg_2SnO_4 sample was also synthesized. Its photoluminescence revealed that the 230 nm

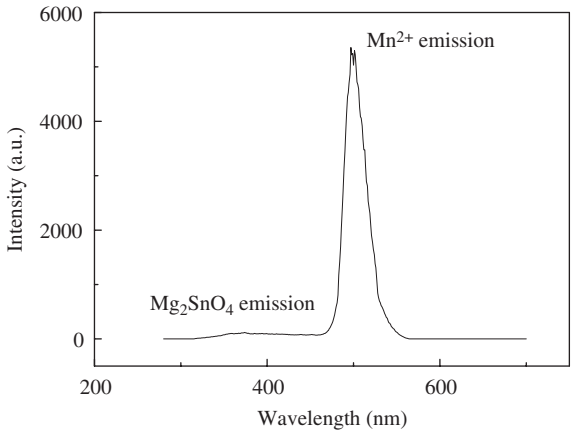

Fig. 2. Emission spectrum of 0.25% Mn^{2+}-doped Mg_2SnO_4 phosphor (excited at 267 nm).

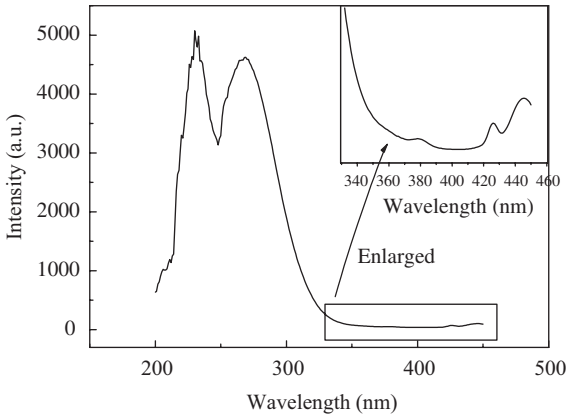

Fig. 3. Excitation spectrum of 0.25% Mn^{2+}-doped Mg_2SnO_4 phosphor monitored at 499 nm.

excitation peak exists in the undoped Mg_2SnO_4 while monitoring the blue emission, indicating that the 230 nm excitation peak belongs to the host absorption. The 267 nm band can be attributed to the absorption of Mn^{2+} ($^6A_{1g}(S)) \rightarrow {}^4A_{1g}(F)$) [23]. In general, there are two channels for luminescence excitation. One is indirect excitation, i.e., excitation into the excited levels of the host, followed by an energy transfer from the host to the impurity ions to yield the luminescence. The other is the direct excitation of the impurity ions. It should be noted that the emission features (positions and profiles) of Mg_2SnO_4:Mn phosphor obtained by indirect (at 230 nm) and direct excitation (at 267 nm) are the same, but the intensity from direct excitation (at 267 nm) is weaker, indicating that luminescence due to the energy transfer from the host is more efficient. The reason for weaker direct absorption is that the Mn^{2+} $d \rightarrow d$ transitions are spin and parity forbidden [23].

3.3. LLP properties of Mg_2SnO_4:Mn^{2+} phosphor

An important result of the present work is that we observed green LLP in the Mg_2SnO_4:Mn^{2+} systems. Fig. 4 represents the afterglow intensity decay curve of the phosphorescence monitored at 499 nm in the 0.25% Mn^{2+}-doped Mg_2SnO_4 phosphor. The afterglow lasted for more than 5 h after removing 254 nm UV irradiatation. To study the decay processes involved in the afterglow, the

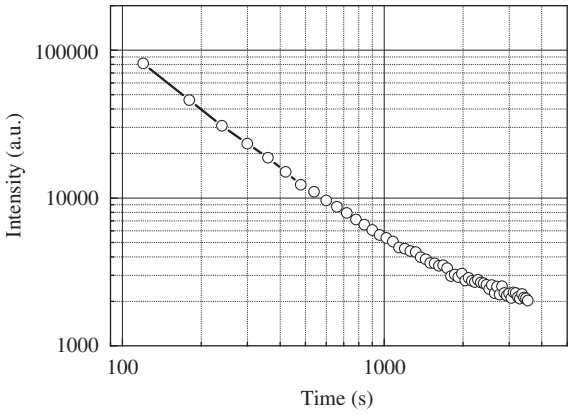

Fig. 4. Afterglow intensity decay curve of the Mg_2SnO_4:0.25% Mn^{2+} phosphor. ($\lambda_{exc} = 254$ nm, $\lambda_{em} = 499$ nm).

decay curve has been analyzed by curve fitting and it was found that the curve can be fitted perfectly using the following exponential equation [26]:

$$I = A_1 \exp(-t/t_1) + A_2 \exp(-t/t_2),$$

where I is the phosphorescence intensity; A_1 and A_2 the two constants; τ is defined as the decay time for the exponential components. The fitting results gave $\tau_1 = 71.1$ and $\tau_2 = 422.9$ s for the two exponential components, respectively. The features of afterglow spectra measured at different decay times (at 2, 5, and 10 min, respectively) were found to be identical and were the same to that of photoluminescence, indicating the same emission centers for both photoluminescence and LLP.

3.4. Possible mechanism of the LLP of Mg_2SnO_4:Mn^{2+} phosphor

Generally, the electronic levels of donor and acceptor of the dopants locate in the host bandgap of LLP materials. First, a luminescent activator serves as an electronic donor that absorbs incident energy. Then the excited electrons move to the trap centers. When these trapped electrons are released by thermal perturbation, LLP takes place [3,25,27]. LLP phenomenon, therefore, is expected from the phosphors if there exist hole traps and electron traps with adequate depths.

Based on the discussion above, it can be assumed that the Mg^{2+} substitution by Mn^{2+} creates appropriate traps where holes or electrons are captured, giving the subsequent radiative recombination with green afterglow emission. The persistent time of the LLP phosphor was affected greatly by the depth and the density of the trap existing in the host. Peaks in the TL curve indicate the depth and the density of traps. Therefore, it is necessary to take the TL spectrum into consideration.

The TL glow curves of different dopant levels in Mg_2SnO_4:Mn^{2+} phosphors are shown in Fig. 5. At least two peaks are clearly observed in all the samples. One peak predominates at 350 K, and another is situated at 460 K. As is shown in the figure, these TL peaks for different dopant levels have the same position but different emission intensity. The 350 K TL peak may originate from the traps created by Mn^{2+} ions located at the tetrahedral Mg^{2+} sites. The equivalent substitution of Mg^{2+} constituent by Mn^{2+} creates isoelectronic traps. The latter 460 K TL peak can be assigned to be related to the Mn^{2+} ions in the octahedral Sn^{4+} sites and the vacancies of Sn^{4+} created during the synthesis process due to the deoxidization of tin oxide component. When Sn^{4+} is replaced by Mn^{2+} ion, two Mn^{2+} ions replace one Sn^{4+} ions to maintain the electroneutrality of the phosphors. To confirm this assignation, Mg_2SnO_4:Mn^{2+} codoped with additional Li^+ phosphors have also been synthesized and their TL properties have also been investigated. The results revealed that the addition of 0.5% Li^+ can

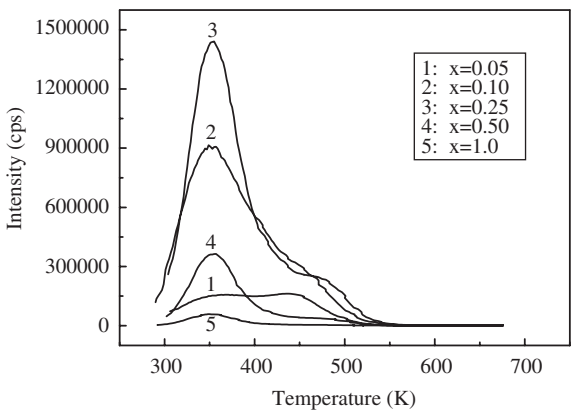

Fig. 5. TL spectra of Mg_2SnO_4:Mn^{2+} phosphor with x mol% of Mn^{2+} ions.

greatly reduce the 460 K TL peak, indicating that the addition of Li^+ ions have significantly reduced the negative $Sn^{\bullet\bullet}_{Mg}$ site impurity trap density. The 350 and 460 K TL peaks have different concentration dependence, this is due to the different distribution of electron/holes among different traps. The trap corresponding to the 350 K TL peak seems to have a greater trapping ability. It is generally believed that the shallower the trap depth is, the lower the temperature of TL peak [5,23,25]. It is also believed that he predominate peaks are situated slightly above room temperature if materials show high LLP performance [5,28,29]. It is clear from Fig. 5 that the traps of $Mg_2SnO_4:Mn^{2+}$ phosphor have appropriate depths. Based on this fact, the addition of Mn^{2+} ion into Mg_2SnO_4 host and the tin and/or oxygen vacancies created in the weak reducing atmosphere are responsible to the green afterglow in this kind of phosphor. Oxygen vacancies may also serve as F-center-like electron traps [17,18]. According to the hole traps, they are probably created by a Mg^{2+} at an Sn^{4+} site in the Mg_2SnO_4 host and the tin vacancies. The released energy due to the recombination of holes and electrons is transferred to the activator ions. Finally, the characteristic activator ions yields afterglow emissions because the energy from the trap has a slow released ratio (shown in Fig. 4).

4. Conclusion

In conclusion, a novel phosphor, $Mg_{2-x}Mn_xSnO_4$, has been synthesized by a conventional solid-state reaction method. Green LLP and PL of the Mn^{2+}-activated material is reported. The LLP can be observed by the naked eyes in dark for over 5 h. The PL and TL properties of materials have been systematically investigated. The optimal PL concentration of $Mg_2SnO_4:Mn^{2+}$ phosphor is found to be 0.25 mol%. The possible mechanisms of phosphorescence have also been discussed.

Acknowledgments

The authors gratefully thank the financial supports by the "One Hundred Talents Project" from the Chinese Academy of Sciences (B. Li and X.J. Wang) and by the National Natural Science Foundations of China (Grant No. 20571071).

References

[1] M. Kowatari, D. Koyama, Y. Satoh, K. Iinuma, S. Uchida, Nucl. Instrum. Methods A 480 (2002) 431.
[2] J. Qiu, K. Miura, H. Inouye, Appl. Phys. Lett. 73 (1998) 1763.
[3] J. Qiu, K. Miura, H. Inouye, S. Fujiwara, T. Mitsuyu, K. Hirao, J. Non-Cryst. Solids 244 (1999) 185.
[4] D. Jia, R.S. Meltzer, W.M. Yen, W. Jia, X. Wang, Appl. Phys. Lett. 80 (2002) 1535.
[5] T. Matsuzawa, Y. Aoki, N. Takeuchi, Y. Murayama, J. Electrochem. Soc. 143 (1996) 2670.
[6] Y. Lin, Z. Tang, Z. Zhang, C. Nan, J. Eur. Ceram. Soc. 23 (2003) 175.
[7] M. Wang, D. Wang, G. Lu, Mater. Sci. Eng. B 57 (1998) 18.
[8] E. Nakazawa, T. Mochida, J. Lumin. 72–74 (1997) 236.
[9] Y.C. Chen, Y.H. Chang, B.S. Tsai, Mater. Trans. 45 (2004) 1684.
[10] K.N. Kim, H.K. Jung, H.D. Park, D. Kim, J. Lumin. 99 (3) (2002) 169.
[11] R.C. Popp, Luminescence and the Solid State, Elsevier, Amsterdam, 1991 291pp.
[12] J.B. Goodnenough, A.L. Loeb, Phys. Rev. 98 (1955) 39.
[13] E.J.W. Verwey, E.L. Heilmann, J. Chem. Phys. 15 (1947) 174.
[14] A.V. Emeline, G.V. Kataeva, V.K. Ryabchuk, N. Serpone, J. Phys. Chem. B 103 (1999) 9190.
[15] T.E. Mitchell, J. Am. Ceram. Soc. 82 (1999) 3305.
[16] R.I. Sheldon, T. Hartmann, K.E. Sickafus, A. Ibarra, B.L. Scott, D.N. Argyriou, A.C. Larson, R.B. Von Dreele, J. Am. Ceram. Soc. 82 (1999) 3293.
[17] D. Jia, W.M. Yen, J. Lumin. 101 (2003) 115.
[18] A. Ibarra, F.J. López, M.J. de Castro, Phys. Rev. B 44 (1991) 7256.
[19] B. Lei, Y. Liu, Z. Ye, C. Shi, Chem. Lett. 32 (2003) 904.
[20] A.M. Azad, L.L.W. Shyan, P.T. Yen, J. Alloys Compounds 282 (1999) 109.
[21] G. Pfaff, Thermochim. Acta 237 (1994) 83.
[22] A.M. Azad, Mater. Res. Bull. 36 (2001) 755.
[23] B. Lei, Y. Liu, Z. Ye, C. Shi, J. Lumin. 109 (2004) 215.
[24] L.E. Shea, R.K. Datta, J.J. Brown Jr., J. Electrochem. Soc. 141 (1994) 1950.
[25] J. Wang, Q. Su, S. Wang, Electrochem. Solid State Lett. 7 (2004) J23.
[26] T. Katsumata, T. Nabae, K. Sasajima, S. Komuro, T. Morikawa, J. Electrochem. Soc. 9 (1997) L243.
[27] C.C. Kang, R.S. Liu, J.C. Chang, B.J. Lee, Chem. Mater. 15 (2003) 3966.
[28] J. Wang, S. Wang, Q. Su, J. Solid State Chem. 177 (2004) 895.
[29] Y. Liu, B. Lei, C. Shi, Chem. Mater. 172 (2005) 2108.